Chapter-4

SELF-STRUCTURIZATION OF SOLAR INTERIOR PLASMA IN REFINED GES-MODEL FRAMEWORK

Abstract: *The self-structurization of realistic polytropic GES-model based bounded solar plasma system is systematically portrayed. It employs a comprehensive study of the electron population behaviours in the SIP, along with electric field and self-gravity gradient variations, in a defined colour phase-space. A dense self-gravity dominated zone is found to emerge from the heliocenter to 0.2* λ_J *in the SIP*[†]*. It hereby confirms the existence of a gravitationally active solar core, as in the SSM, as per our model analysis.*

4.1 INTRODUCTION

The solar plasma system as a whole has been a complex laboratory in nature to explore various plasma constituent structurization processes in diverse environments. A most challenging and striking problem in this direction is the role of thermo-statistical behaviour of the constitutive tiny electrons on the flow dynamics, and hence self-organization of the non-thermal solar plasma medium [1-3].

It is seen in the available literature that the structure of the solar interior has been well modelled following the widely accepted standard solar model (SSM) in the past [4-6]. However, the equilibrium spatial material distribution of the solar interior plasma (SIP) medium in the realistic polytropic gravito-electrostatic sheath (GES)-model framework has never been explored before. Consequently, with this motivation behind, the present chapter is devoted to illuminate the role of the various electronic non-thermality extents in formation of distinct SIP structures of the solar plasma system as per the polytropic turbulent magneto-active GES-model fabric.

4.2 PHYSICAL MODEL FORMULATION

The solar plasma medium is assumed to be composed of lighter non-thermal electrons following κ-distribution and heavier gravitating inertial ions following the principles of

[†]Sarma, P. and Karmakar, P. K. Solar plasma characterization in Kappa (κ)-modified polytropic turbomagnetic GES-model perspective. *Monthly Notices of the Royal Astronomical Society*, 519(2):2879-2916, 2023.

fluid dynamics. The solar plasma system is taken as spherically symmetric, making the variables only radially dependent, and the polar and azimuthal counterparts fully relaxed [4, 5]. The realistic magneto-activity and turbulence effects are judiciously incorporated into the equation of state [7, 8]. All the key physical insights behind the sheath formation are well explained in previously reported literatures [9] as well as in previous chapters. Accordingly, all the model governing equations are well presented below in their normalized time-stationary form for studying the equilibrium solar configuration.

The equations here represent the solar interior plasma system and the external boundary of the bounded solar structure is determined by the exact balancing of the self-gravitational and electrostatic force fields. The set of the basic governing equations of the bounded SIP consists of the electronic κ-distribution function, continuity and momentum equations representing ion dynamics, equation of state, Poisson equation for gravitational and electrostatic fields, and the electric current density evolution equation. The significances of the symbols and the normalization scheme are detailed in Tables 2.1 and 2.2 respectively. Consequently, the normalized equations are expressed as follows.

The κ-distribution law followed by electron population density is expressed as

$$N_e = \left[1 - \left(\frac{2}{2\kappa - 3}\right)\Phi\right]^{-\kappa+1/2}. \quad (4.1)$$

The ion continuity equation following ionic mass conservation is given as

$$M\left(\partial_\xi N\right) + N\left(\partial_\xi M\right) + \left(\frac{2}{\xi}\right) M\, N = 0. \quad (4.2)$$

The ion momentum equation following ionic linear momentum conservation is written as

$$\begin{aligned} M\left(\partial_\xi M\right) = & -T_e^*\left(\partial_\xi \Phi\right) - \left(\frac{\alpha \lambda_J \Gamma n_0^{\Gamma-1}}{m_i c_s^2}\right) N^{\Gamma-2}\left(\frac{2\kappa-1}{2\kappa-3}\right)\left[1-\left(\frac{2}{2\kappa-3}\right)\Phi\right]^{-\kappa-1/2}\frac{1}{\lambda_J}\left[\partial_\xi \Phi + T_e^* \Phi\, \partial_\xi\left(\frac{1}{T_e^*}\right)\right] \\ & -\frac{1}{N}\left[T_i^*\left(\partial_\xi N\right) + N\left(\partial_\xi T_i^*\right)\right]\left[1+\ln(N)\right] - T_i^*\frac{1}{N}\left(\partial_\xi N\right) - \partial_\xi \Psi + \left(\frac{\eta}{m_i n_0 c_s \lambda_J}\right)\frac{1}{\xi^2}\frac{1}{N}\left[\partial_\xi\left(\xi^2\, \partial_\xi M\right)\right] \end{aligned}. \quad (4.3)$$

The realistically modified equation of state is expressed as

$$P_T^* = \left(\frac{\alpha\, n_0^\Gamma}{P_0}\right)\left[1-\left(\frac{2}{2\kappa-3}\right)\Phi\right]^{(-\kappa+1/2)\Gamma} + P_{Th}^*\left[1 + ln\left(N_i\right)\right] + \beta_0\left(B^*\right)^2. \quad (4.4)$$

The electrostatic Poisson equation for the electric potential distribution is written as

$$N_e - N_i = \left(\frac{\lambda_{De}}{\lambda_J}\right)^2\left[\partial_\xi^2 \Phi + \left(\frac{2}{\xi}\right)\partial_\xi \Phi\right]. \quad (4.5)$$

The gravitational Poisson equation showing the self-gravitational potential distribution in the SIP mass is given by

$$\partial_\xi^2 \Psi + \left(\frac{2}{\xi}\right)\partial_\xi \Psi = N \,. \tag{4.6}$$

The current density evolution equation in the SIP is cast as

$$J_{SIP} = N\left[-\sqrt{2\,\xi\,(\partial_\xi \Psi)} - \sqrt{\left\{2\left(\frac{T_e}{T_i}\right)\xi\left(\partial_\xi \Phi\right)\right\}} + \sqrt{\left\{2\left(\frac{m_i}{m_e}\right)\left(\frac{T_e}{T_i}\right)\xi\left(\partial_\xi \Phi\right)\right\}}\right]. \tag{4.7}$$

The above equations are coupled to get a set of basic first order time-stationary differential equations. The fourth-order Runge-Kutta (RK-IV) method is applied with initial input values as depicted in Table 2.3 for numerical analysis, and hence obtaining the various significant plots for studying the self-structurization of the bounded solar plasma constituents [10].

4.3 RESULTS AND DISCUSSIONS

In order to explore the self-organization of the SIP medium, at first the formation of the edge of the SIP is observed for different electronic non-thermality levels (as indicated by the κ-value). It is well portrayed in figure 4.1. A bi-scaled solar plasma system that is the SIP and the solar wind plasma (SWP) is formed, differentiated by the interfacial solar surface boundary (SSB). The SSB lies at the location of exact gravito-electrostatic force balancing.

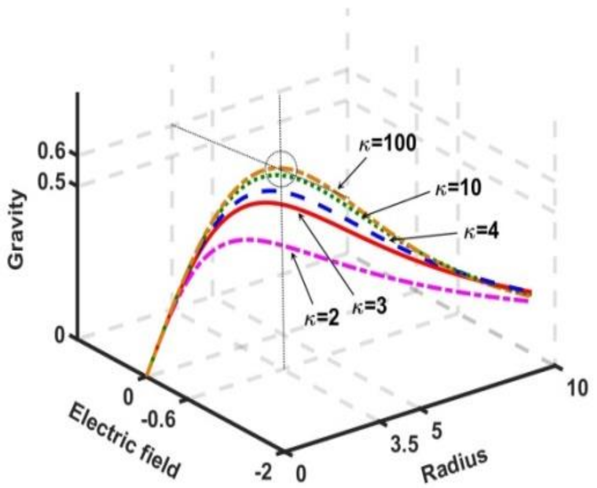

Figure 4.1: *Profile of the normalized gravitational field (gravity) strength with variation in the Jeans-normalized heliocentric radial distance and electric field strength for different κ-values highlighting the radial SSB-location.*

It is clear that the SIP shrinks with an increase in the electron non-thermal behaviour (i.e., decreasing κ-value). The physics behind is explained in **Chapter-2**. Now the self-organization of the material inside the SIP is studied as explained below.

In figure 4.2, we depict the colour-spectral profile of the normalized electron number density with the variation in the normalized electric potential and gravitational field strength for different κ-values in 2D and 3D graphical forms for a clear portrayal of the SIP structure. It is observed that the electrons have a tendency to lie in the zero-potential region (that is near the heliocenter, as seen previously in figure 2.2). This behaviour intensifies with an increase in the electron thermality. As the SIP volume shrinks with an increase in the electron non-thermality, the mutual electronic repulsion in the solar core causes them to disperse away outwards.

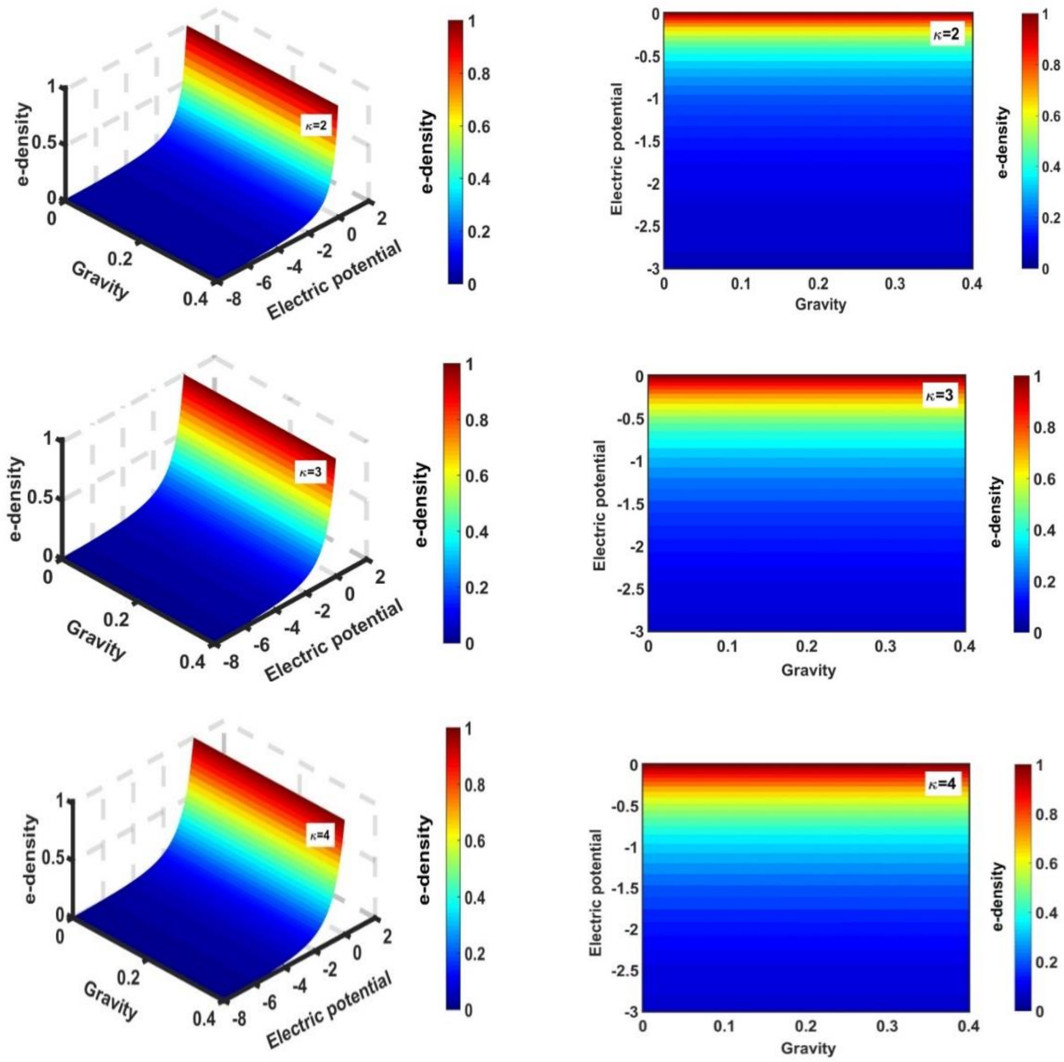

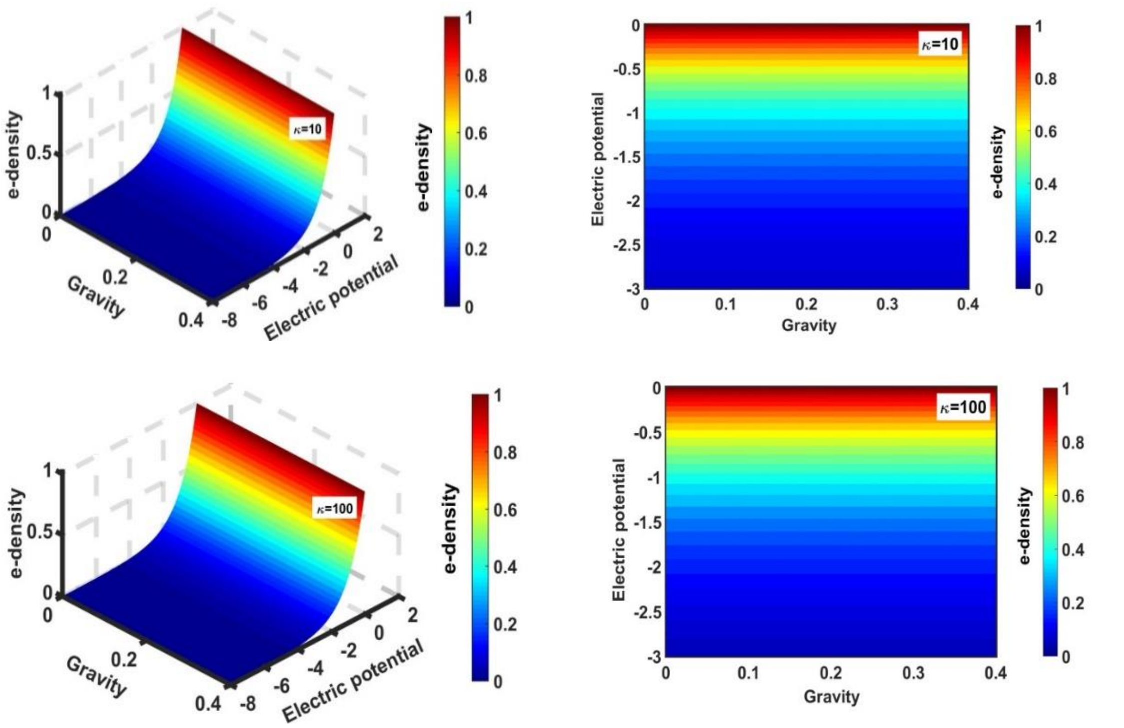

Figure 4.2: *Colour-spectral profile of the normalized electron number density (e-density) with variation in the normalized electric potential and gravitational field strength (gravity) for different degrees of the electron non-thermality (indicated with κ).*

In figure 4.3, we represent the colour-spectral profile of the normalized electric field gradient strength following the variation in the electric field strength and the Jeans-normalized heliocentric radial distance for different κ-values in 2D and 3D shapes. It is seen that the field gradient is independent of the electron non-thermality. A distinct transition in the electric field gradient is noticed at a radial distance of 0.2 λ_J. The magnitude of the electric field gradient rises significantly with rise in the electric field strength, from the heliocenter to 0.2 λ_J, but not so beyond that region. This behaviour indicates a very highly dense self-gravity dominant zone in the SIP, in which an intense electric field gradient is of utmost importance to beat the electrostatic shielding effect between the oppositely polar constitutive charged solar plasma species.

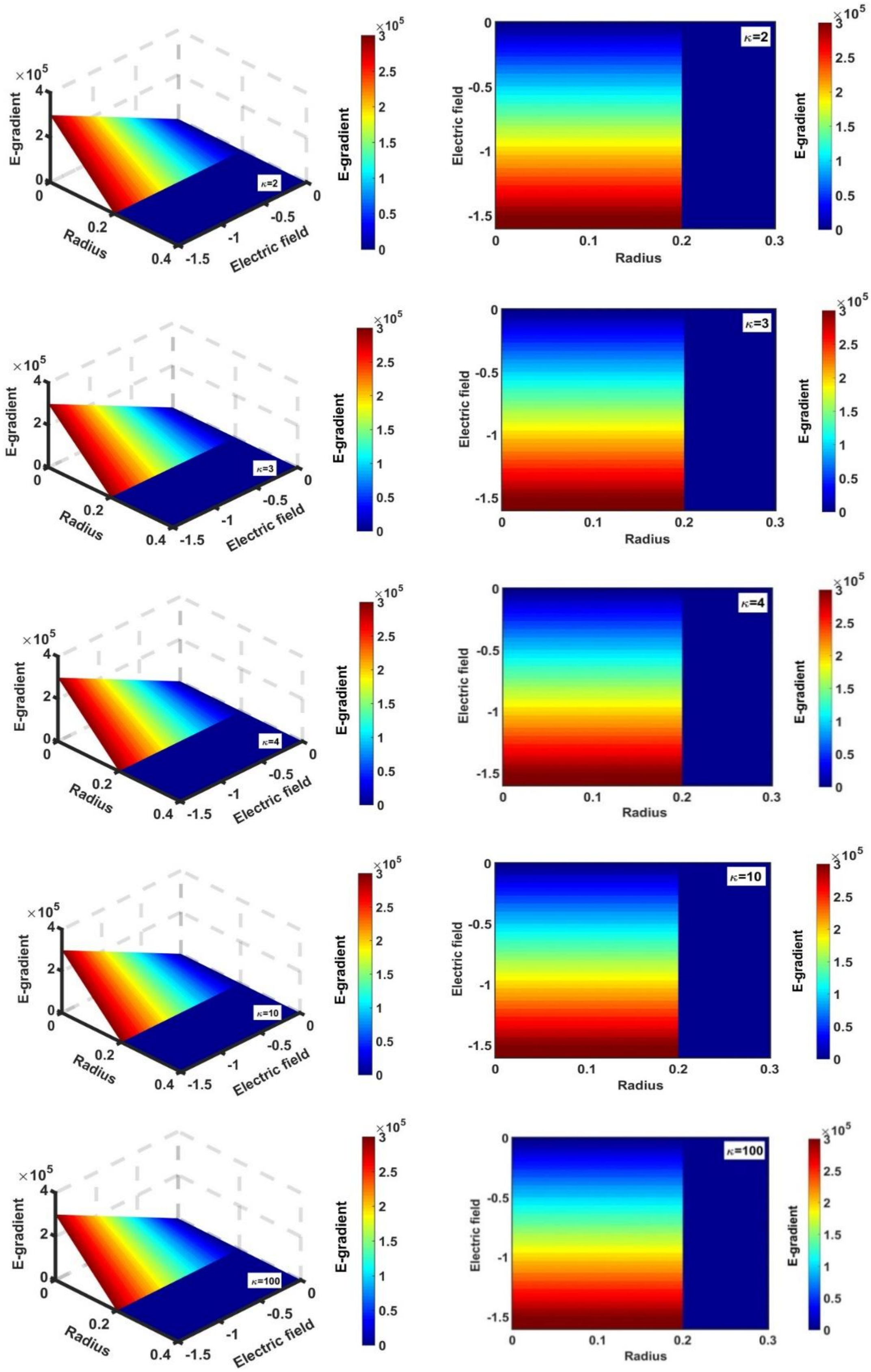

Figure 4.3: *Colour-spectral profile of the normalized electric field strength gradient (E-gradient) with variation in the normalized electric field strength and heliocentric radial distance for different degrees of the electron non-thermality (as indicated with κ).*

As in figure 4.4, we portray the colour-spectral profile of the normalized self-gravitational field gradient strength following the variation in the self-gravitational strength and the Jeans-normalized heliocentric radial distance for different κ-values in 2D and 3D patterns. It is seen that the magnitude of the self-gravity gradient increases with an increase in the electron thermality. But this behaviour is noticed only in the region confined between the heliocenter and $\xi = 0.2\ \lambda_J$. This behaviour is attributable to the fact of the increasing SIP volume (or decreasing density) with the electron thermality. If the core becomes rarer, the associated self-gravity gradient must have a high magnitude to attain the corresponding non-zero gravity strength. For a high electron non-thermality, the core density increases due to decrease in the SIP volume, which facilitates the attainment of high-gravity strength even without a need of a high self-gravity gradient in that region of the SIP.

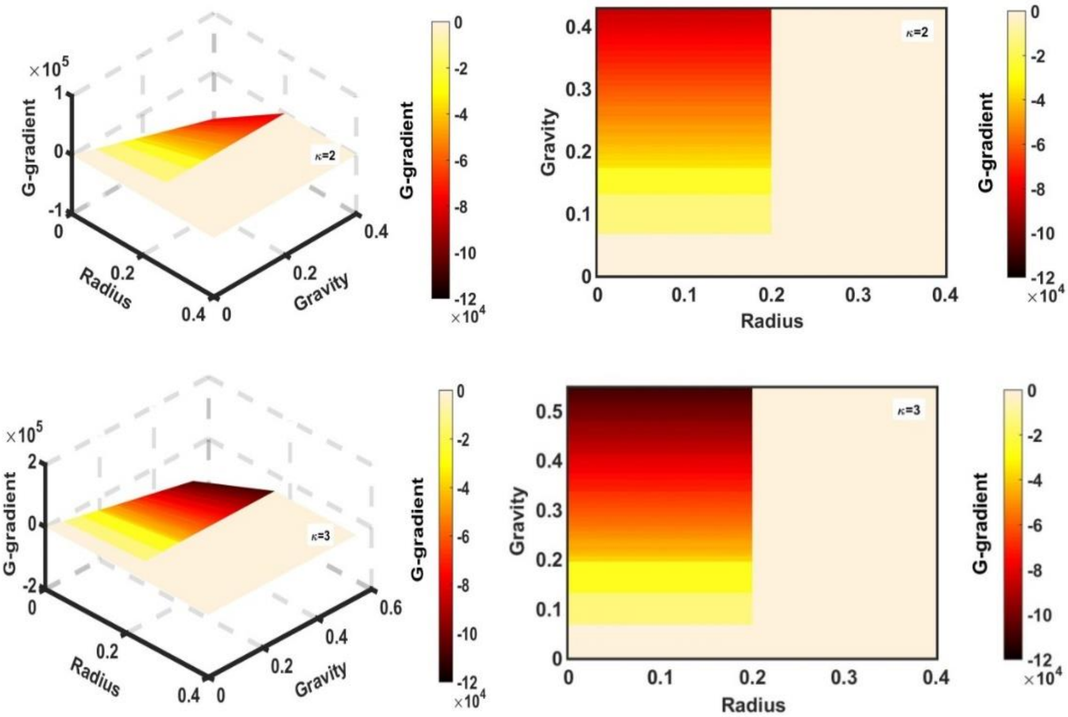

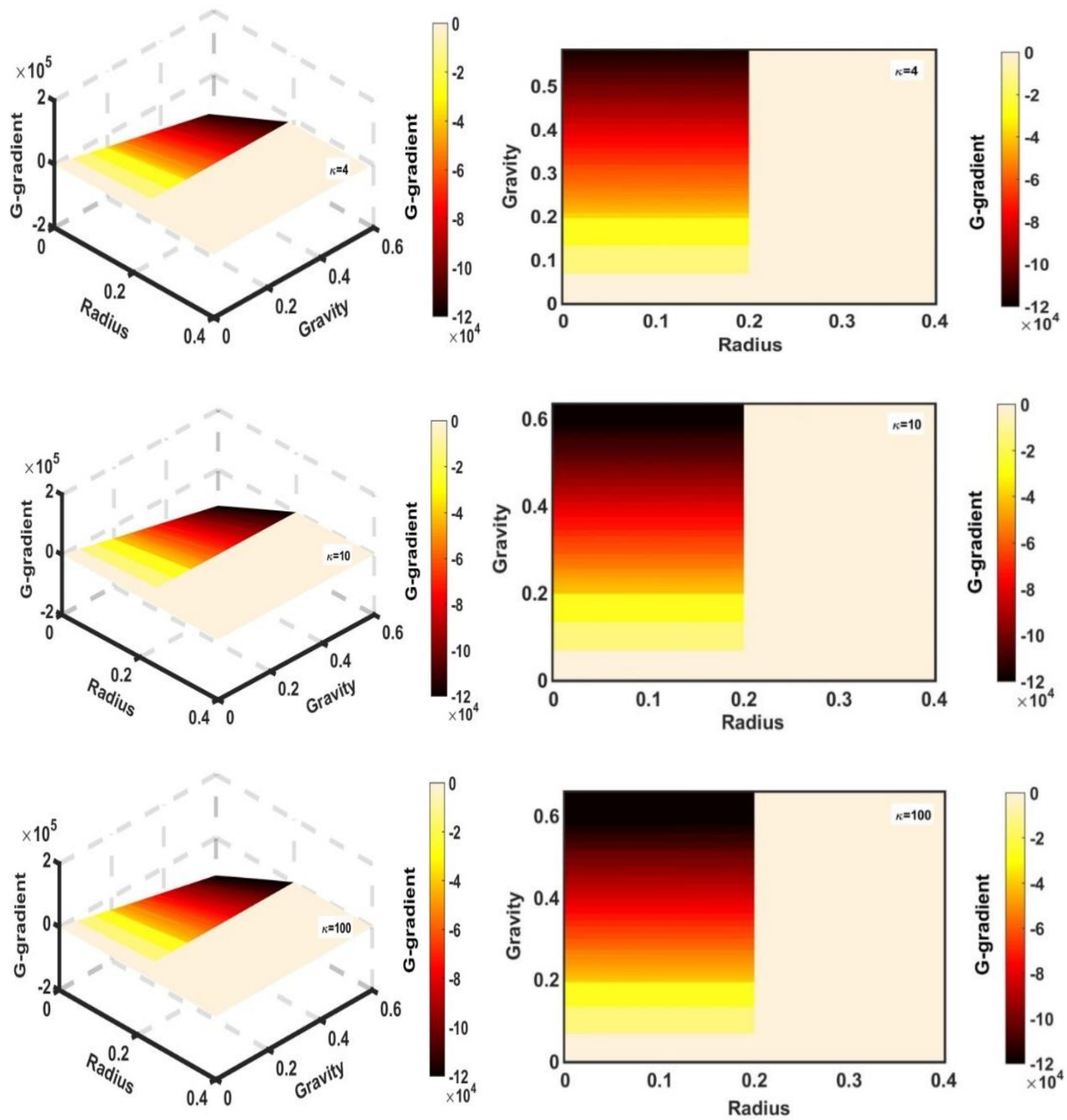

Figure 4.4: *Colour-spectral profile of the normalized self-gravitational field strength gradient (G-gradient) with variation in the normalized self-gravitational field strength (gravity) and heliocentric radial distance for different degrees of the electron non-thermality (as indicated with κ).*

From figures 4.3-4.4, we infer that the SIP structurizes itself into a highly dense sharply defined self-gravity dominant zone, which is independent of the electron non-thermality. This is an interesting unique outcome of our presented GES-model formalism alone for the first time. This outcome (i.e., the dense region within heliocenter and ξ = 0.2 λ_J = 4 × 10^7 m) stands well with the SSM, which predicts that the highly dense core lies from the heliocenter to a radial distance of 2.09 ×10^8 m [11].

4.4 CONCLUSIONS

The internal structure and organization of the SIP in the GES-model based solar plasma system is re-examined with the incorporation of various realistically sensible factors, but previously remaining unincorporated in the same context. It includes the plasma-electron non-thermality effects (via the κ-distribution law), magnetic pressure (via the Lorenz force action), and plasma fluid turbulence (via the Larson logatropic equation of state). The self-structurization of the confined solar constitutive plasma fluid is illuminated by looking into the behaviours of the electron population (figure 4.2), and the electric and self-gravity field gradients with their field values against the heliocentric radial distance in a defined colour-spectral portrayal form (figures 4.3-4.4).

It is found that the electrons have a tendency to lie in the heliocentric region; this nature intensifies with an increase in the electron thermality. It is due to negligible potential of the heliocentric region. As the SIP shrinks with an increase in the electron non-thermality, the mutual electronic repulsion in the core causes their outward dispersion. The magnitude of the electric field gradient rises significantly with rise in the electric field strength, from the heliocenter to a radial distance of 0.2 λ_J, but not so beyond. The magnitude of self-gravity gradient increases with an increase in the electron thermality effects. It is due to the SIP expansion with an increase in the electronic thermality. But this behaviour is noticed only in the region confined between the above radial points. A highly dense and sharply defined self-gravity dominated region is clearly revealed for the first time to exist from the heliocenter to 0.2 λ_J. This outcome as per our present model analysis stands fairly in conformity with the SSM-based predictions.

REFERENCES

[1] Pierrard, V. and Lazar, M. Kappa distributions: theory and applications in space plasmas. *Solar Physics*, 267, 153:153-174, 2010.

[2] Livadiotis, G. and McComas, D. J. Understanding kappa distributions: a toolbox for space science and astrophysics. *Space Science Reviews*, 175:183–214, 2013.

[3] Yoon, P. H., Sarfraz, M., Ali, Z., Salem, C. S., and Seough, J. Proton cyclotron and mirror instabilities in marginally stable solar wind plasma. *Monthly Notices of the Royal Astronomical Society*, 509(4):4736-4744, 2022.

[4] Stix, M. *The Sun: An Introduction*. Springer, Berlin, 1991.

[5] Priest, E. *Magnetohydrodynamics of the Sun*. Cambridge University Press,

Cambridge, New York, 2014.

[6] Kippenhahn, R., Weigert, A., and Weiss, A. *Stellar Structure and Evolution*. Springer, Berlin, 2012.

[7] Chen, F. F. *Introduction to Plasma Physics and Controlled Fusion*. Springer, New York, 1984.

[8] Vazquez-Semadeni, E., Canto, J., and Lizano, S. Does turbulent pressure behave as a logatrope? *Astrophysical Journal*, 492:596-602, 1998.

[9] Dwivedi, C. B., Karmakar, P. K., and Tripathy, S. C. A gravito-electrostatic sheath model for surface origin of subsonic solar wind plasma. *Astrophysical Journal*, 663:1340-1353, 2007.

[10] Sarma, P. and Karmakar, P. K. Solar plasma characterization in Kappa (κ)-modified polytropic turbomagnetic GES-model perspective. *Monthly Notices of the Royal Astronomical Society*, 519(2):2879-2916, 2023.

[11] Carroll, W. and Ostlie, D. A. *An Introduction to Modern Astrophysics*. Cambridge, UK, 2017.